

ARTICLES

Structure and stability of strange and charm stars at finite temperatures

Ch. Kettner, F. Weber,* and M. K. Weigel

Institute for Theoretical Physics, University of Munich, Theresienstrasse 37/III, 80333 Munich, Germany

N. K. Glendenning

Nuclear Science Division, Lawrence Berkeley Laboratory, MS: 70A-3307, Berkeley, California 94720

(Received 29 August 1994)

This paper consists of four parts. Part one deals with an investigation of the properties of β -equilibrated, electrically charged neutral quark-star matter at zero and finite temperatures, and the determination of its equation of state. In part two, the properties of sequences of quark stars, divided into strange- and charm-quark stars, depending on quark-flavor content, are investigated. The strange stars are constructed for absolutely stable strange-quark matter, whose energy per baryon number lies below the one in ^{56}Fe . In part three, the electrostatic potential of electrons inside and in the close vicinity outside of strange stars, which is of decisive importance for the possible existence of nuclear crusts on the surfaces of such stars, is computed. It is found that finite temperatures lead to a considerable reduction of the electrostatic electron potential at the surface of a strange star, which is accompanied by a strong reduction of the Coulomb barrier associated with the difference of the electrostatic potential at the surface of the star's strange-matter core and the base of the crust. This finding is of great importance for the stable existence of crusts on strange stars, since the Coulomb barrier plays the important role of preventing atomic nuclei bound in the nuclear crust from coming into contact with the star's strange-matter core, where atomic matter by hypothesis would be converted into strange matter. The structure and stability of quark stars against radial oscillations is discussed in part four, where it is found that charm-quark stars are unstable against radial oscillations. Thus no charm-quark stars (and, as is demonstrated too, no quark-matter stars possessing still higher central mass densities) can exist in nature.

PACS number(s): 97.10.Cv, 97.10.Nf, 97.60.Gb, 97.60.Jd

I. INTRODUCTION

The hypothesis that strange quark matter may be the absolute ground state of the strong interaction (i.e., absolutely stable with respect to ^{56}Fe) has been raised by Bodmer [1] and Witten [2]. On theoretical scale arguments, it is as plausible a ground state as the confined state of hadrons [2–4]. Even to the present day there is no sound scientific basis on which one can either confirm or reject Witten's hypothesis, so that it remains a serious possibility of fundamental significance for rare but exotic phenomena [5–12]. (For a review of recent work, and a complete bibliography up to 1991, see Ref. [13].) If the hypothesis is true, then the very intriguing possibility of the existence of so-called *strange*-quark matter stars

[2,4,11,14–17], made up of 3-flavor strange-quark matter whose energy per baryon number lies below the one of ^{56}Fe , i.e., 930 MeV, opens up. They form a distinct and disconnected branch of compact stars, and are not part of the continuum of equilibrium configurations that include white dwarfs and neutron stars [2,4,14,15]. More than that, some (in the most extreme case all) neutron stars could actually be strange stars. If so, pulsars are to be interpreted as rotating strange stars (strange pulsars) rather than rotating neutron stars [13]. Possible signatures of such objects could be rotational pulsar periods that lie significantly below one millisecond [9,18], since the rotational periods of gravitationally bound neutron stars, constructed for a broad collection of realistic models for the nuclear equation of state, seem to lie above that limit [19–22].

This paper deals with an investigation of the properties of quark-star matter at zero as well as nonzero temperatures, and the determination of the equation of state (i.e., pressure versus energy density relation) associated with it. The notion of quark-star matter comprises

*Also at Nuclear Science Division, Lawrence Berkeley Laboratory, MS:70A-3307, Berkeley, CA 94720.

strange-quark star matter made up of u , d , and s quarks [2,4,11,14–17] and *charm-quark* star matter [23], in which charm-quark states are populated in addition. Subsequently, the properties of the families of strange- and charm-matter stars, henceforth referred to, for brevity, as *strange* and *charms stars*, constructed for these equations of state are analyzed. There exist a few investigations dealing with the properties of strange stars that have been performed earlier than this one (for an overview, see, for example, Ref. [13]). Some of the major new aspects treated in this work concern the investigation of the structure and stability of strange and charm stars, being at zero as well as nonzero temperatures, against radial oscillations. Furthermore, the influence of temperature on the electron chemical potential inside and outside of bare strange stars, which is of decisive importance for the possible existence of nuclear crusts on the surfaces of strange stars, is explored and its implications for strange pulsars are pointed out. The investigation is based on a systematic determination of a model for the equation of state of quark-star matter at finite temperature, whose properties are studied in great detail.

Our investigation is organized as follows. In Sec. II the description of quark-*star* matter, i.e., β -equilibrated three- (u, d, s) and four-flavor (u, d, s, c) quark matter, at zero as well as finite temperatures is introduced. For the purpose of illustration, the special cases of cold quark matter made up of massless as well as massive quarks are discussed. A value for the bag constant of $B^{1/4} = 145$ MeV, for which 3-flavor strange-quark matter is stable, has been chosen. For a strange quark mass of 150 MeV, this bag constant corresponds to an equilibrium energy per baryon number of strange matter of about 880 MeV. In other words, this choice represents strange matter being absolutely bound, by about 50 MeV, with respect to ^{56}Fe . Sequences of strange- and charm-quark stars are constructed in Sec. III. In particular, the impact of temperature on the structure of such objects is investigated. In Sec. IV the electrostatic potential of electrons interior and exterior of strange stars is determined and its temperature dependence studied. Most important for the possible existence of a nuclear crust on the surface of a strange star, the width of the gap that exists between the surface and the base of the crust is determined for a variety of representative temperatures and electrostatic crust potentials. As a by-product, the possibility of the conversion of hadronic matter (light atomic nuclei, such as hydrogen and helium) that is accreted onto the surface of a bare strange star into strange matter is considered. Section V deals with an investigation of the stability of such stars against radial oscillations (acoustical modes). Our findings are summarized in Sec. VI. Mathematical details concerning the determination of the equation of state at finite temperature are given in the Appendix.

II. DESCRIPTION OF QUARK-STAR MATTER

In the following we present briefly the description of electrically charge neutral quark-star matter in equilibrium with respect to the weak interactions (i.e., β -stable

matter) at zero as well as finite external pressure and non-zero temperature. By quark-star matter we mean a Fermi gas of $3A$ quarks which together constitute a single color-singlet baryon with baryon number A . The dynamics of quark confinement is approximated by the bag model [24]:

$$p + B = \sum_{i=u,d,c,s;e^-, \mu^-} p_i, \quad (2.1)$$

$$\epsilon = \sum_{i=u,d,c,s;e^-, \mu^-} \epsilon_i + B, \quad (2.2)$$

where p , ϵ , and B refer to external pressure, total internal energy density, and bag constant, respectively. The condition of electric charge neutrality reads

$$0 = \sum_{i=u,d,c,s;e^-, \mu^-} q_i n_i. \quad (2.3)$$

The expressions for internal pressure, energy, and number density of the quarks and leptons contained in the bag, p_i , ϵ_i , and n_i respectively, are determined by the thermodynamic potentials, $d\Omega_i = -S_i dT - P_i dV - N_i d\mu_i$, from which one obtains [contributions of antiparticles are neglected; this is well justified for antiquarks since their chemical potentials are much larger than the considered temperatures (see also [25]); the situation is somewhat more delicate for the positrons, which too were found to contribute only very little]

$$\omega_i = \frac{\partial \Omega_i}{\partial V} = -\frac{g_i T}{2\pi^2} \int_0^\infty dk k^2 \ln [1 + e^{-(E_i(k) - \mu_i)/T}], \quad (2.4)$$

$$p_i = -\omega_i = \frac{g_i}{6\pi^2} \int_{m_i}^\infty dE (E^2 - m_i^2)^{3/2} f_i(E), \quad (2.5)$$

$$n_i = -\frac{\partial \omega_i}{\partial \mu_i} = \frac{g_i}{2\pi^2} \int_{m_i}^\infty dE E \sqrt{E^2 - m_i^2} f_i(E), \quad (2.6)$$

where $E_i^2(k) \equiv k^2 + m_i^2$. (For the evaluation of the thermodynamic potential of a quark gas of N_c colors and N_f flavors to fourth order in the quark-gluon coupling, we refer to Refs. [26,27].) The quantity m_i denotes the quark's mass. The expression for the energy density of the system reads

$$\epsilon_i = \frac{g_i}{2\pi^2} \int_{m_i}^\infty dE E^2 \sqrt{E^2 - m_i^2} f_i(E). \quad (2.7)$$

The phase space factor g_i is equal to 2 (leptons) or 6 (quarks). The quantity f_i denotes the Fermi-Dirac distribution function, $f_i(E) \equiv 1/\{1 + \exp[(E - \mu_i)/T]\}$. The baryon number density is given by

$$n_A = \frac{1}{3} \sum_{i=u,d,s,c} n_i. \quad (2.8)$$

Chemical equilibrium between the quark flavors and the leptons is maintained by the weak reactions (and their inverse)

$$d \longrightarrow u + e^- + \bar{\nu}_{e^-} , \quad (2.9)$$

$$s \longrightarrow u + e^- + \bar{\nu}_{e^-} , \quad (2.10)$$

$$s \longrightarrow c + e^- + \bar{\nu}_{e^-} . \quad (2.11)$$

The reactions

$$s + u \longleftrightarrow d + u , \quad (2.12)$$

$$c + d \longleftrightarrow u + d , \quad (2.13)$$

contribute to the equilibration of flavors. The loss of neutrinos by the star implies that their chemical potential is equal to zero. Hence, one gets from Eqs. (2.9)–(2.13)

$$\mu_d = \mu_u + \mu_{e^-} , \quad \mu_c = \mu_u , \quad \mu_s = \mu_u . \quad (2.14)$$

Finally, the conservation of electric charge implies that

$$\mu_{e^-} = \mu_{\mu^-} . \quad (2.15)$$

The third of Eq. (2.14) motivates defining

$$\mu \equiv \mu_d = \mu_s . \quad (2.16)$$

For later purpose, we introduce the additional definitions

$$\eta_i \equiv \frac{\mu_i}{\mu} = \begin{cases} 1-x & \text{if } i = u, c , \\ 1 & \text{if } i = d, s , \\ x & \text{if } i = e^-, \mu^- , \end{cases} \quad (2.17)$$

where

$$x \equiv \frac{\mu_{e^-}}{\mu} \quad \text{and} \quad z_i \equiv \frac{m_i}{\eta_i \mu} = \frac{m_i}{\mu} . \quad (2.18)$$

A. Cold matter consisting of massless quarks

It is illustrative to apply, in a first step, the equations of the previous section to quark matter at zero temperature, assuming that all quark species are massless particles. Zero temperature implies that

$$f_i(E) \xrightarrow{T \rightarrow 0} \Theta(\mu_i - E) , \quad (2.19)$$

and Eqs. (2.4)–(2.7) lead to ($g_i = 6$)

$$p_i = \frac{g_i}{24\pi^2} \mu^4 \eta_i^4 = \frac{1}{3} \epsilon_i , \quad (2.20)$$

$$n_i = \frac{g_i}{6\pi^2} \mu^3 \eta_i^3 . \quad (2.21)$$

One thus obtains from Eqs. (2.1) and (2.2) for the system's equation of state the well known expression

$$p = \frac{\epsilon - 4B}{3} . \quad (2.22)$$

The condition of charge neutrality, Eq. (2.3), reads

$$\frac{2}{3} n_u - \frac{1}{3} (n_d + n_s) = 0 , \quad (2.23)$$

(no leptons are necessary to make the system electrically charge neutral). Finally, for zero external pressure, $p = 0$, one derives from Eq. (2.1) $B = 3\mu^4/4\pi^2$, and for the energy per baryon number in strange matter [11],

$$E_A \equiv \frac{\epsilon}{n_A} = \frac{4B}{(n_u + n_d + n_s)/3} = \frac{4B}{n_u} = \frac{4B\pi^2}{\mu^3} . \quad (2.24)$$

From this relation one finds, for example, that bag constants of $B = 57.5 \text{ MeV/fm}^3$ ($B^{1/4} = 145 \text{ MeV}$) and $B = 85.3 \text{ MeV/fm}^3$ ($B^{1/4} = 160 \text{ MeV}$) place the energy per baryon number of strange matter consisting of *massless* u , d , and s quarks at 829 MeV and 915 MeV, respectively. In other words, these values represent strongly ($\sim 100 \text{ MeV}$) and weakly ($\sim 15 \text{ MeV}$) bound strange matter, at zero external pressure, and in all cases correspond to strange matter being absolutely bound with respect to ^{56}Fe . (More details will be given in connection with the discussion of Figs. 1 and 2.)

B. Cold matter consisting of massive quarks

In the case of massive quarks, Eqs. (2.5)–(2.7) lead to ($i = u, d, c, s; e^-, \mu^-$)

$$p_i = \frac{g_i \mu^4 \eta_i^4}{24\pi^2} \left[\sqrt{1 - z_i^2} \left(1 - \frac{5}{2} z_i^2\right) + \frac{3}{2} z_i^4 \ln \frac{1 + \sqrt{1 - z_i^2}}{z_i} \right] , \quad (2.25)$$

$$n_i = \frac{g_i \mu^3 \eta_i^3}{6\pi^2} (1 - z_i^2)^{\frac{3}{2}} , \quad (2.26)$$

$$\epsilon_i = \frac{g_i \mu^4 \eta_i^4}{8\pi^2} \left[\sqrt{1 - z_i^2} \left(1 - \frac{1}{2} z_i^2\right) - \frac{z_i^4}{2} \ln \frac{1 + \sqrt{1 - z_i^2}}{z_i} \right] . \quad (2.27)$$

The condition of electric charge neutrality, Eq. (2.3), reads now

$$0 = \frac{2}{3} (n_u + n_c) - \frac{1}{3} (n_d + n_s) - (n_{e^-} + n_{\mu^-}) , \\ = 2(1 - x^3) [1 + (1 - z_c^2)^{\frac{3}{2}}] - [1 + (1 - z_s^2)^{\frac{3}{2}}] - x^3 [1 + (1 - z_{\mu^-}^2)^{\frac{3}{2}}] , \quad (2.28)$$

and Eq. (2.1) leads to

$$\frac{(p + B) 4\pi^2}{\mu^4} = (1 - x^4) \left[1 + \sqrt{1 - z_c^2} \left(1 - \frac{5}{2} z_c^2\right) + \frac{3}{2} z_c^4 \ln \frac{1 + \sqrt{1 - z_c^2}}{z_c} \right] \\ + \left[1 + \sqrt{1 - z_s^2} \left(1 - \frac{5}{2} z_s^2\right) + \frac{3}{2} z_s^4 \ln \frac{1 + \sqrt{1 - z_s^2}}{z_s} \right] + \frac{x^4}{3} \left[1 + \sqrt{1 - z_{\mu^-}^2} \left(1 - \frac{5}{2} z_{\mu^-}^2\right) + \frac{3}{2} z_{\mu^-}^4 \ln \frac{1 + \sqrt{1 - z_{\mu^-}^2}}{z_{\mu^-}} \right] . \quad (2.29)$$

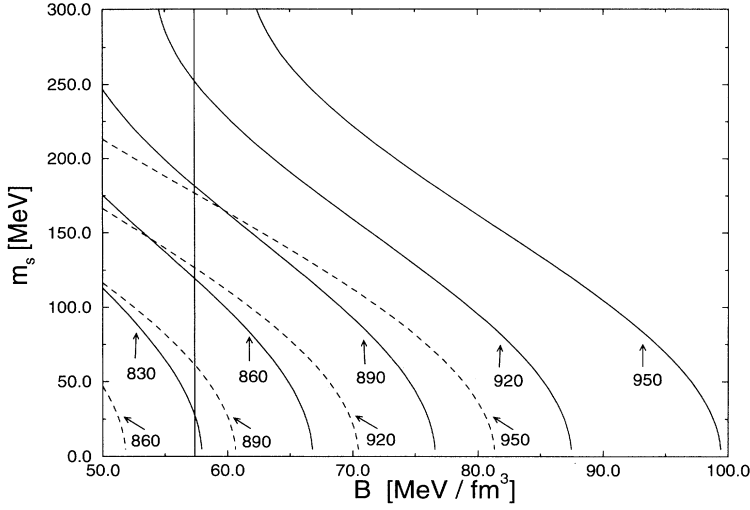


FIG. 1. Contours of fixed energy per baryon number (figures attached to these curves) of strange quark matter at zero external pressure. The solid and dashed curves refer to $T = 0$ and $T = 30$ MeV, respectively. The strange quark mass is plotted on the y axis and the bag constant B on the x axis.

The expressions of energy and baryon number density are given by

$$\epsilon = 3p + 4B + \sum_{i=s,c,\mu^-} \epsilon_i - 3 \sum_{i=s,c,\mu^-} p_i \quad (2.30)$$

$$\begin{aligned} &= 3p + 4B \\ &+ \sum_{i=s,c,\mu^-} \frac{g_i \mu_i^4 \eta_i^4}{4\pi^2} z_i^2 \left[\sqrt{1 - z_i^2} - z_i^2 \ln \frac{1 + \sqrt{1 - z_i^2}}{z_i} \right] \end{aligned} \quad (2.31)$$

and

$$\begin{aligned} n_A &= \frac{1}{3} (n_u + n_d + n_s + n_c) \\ &= \frac{\mu^3}{3\pi^2} \left[(1 - x^3)(1 + (1 - z_c^2)^{\frac{3}{2}}) + (1 + (1 - z_s^2)^{\frac{3}{2}}) \right]. \end{aligned} \quad (2.32)$$

The first two terms on the right-hand side of Eq. (2.31)

represent the equation of state of massless quarks, given by Eq. (2.22). The third term accounts for the finite masses of the muons, and the strange and charm quarks.

Figure 1 shows the energy per baryon number, $E_A = \epsilon/n_A$, of strange matter at zero external pressure [3,25], computed from Eq. (2.31). The influence of temperature is demonstrated for $T = 30$ MeV, which is typical for a newly formed neutron star in a supernova explosion [28–30]. (The equation of state of quark-star matter at finite temperature will be discussed in detail in Sec. II C.) The energy per baryon number of cold matter ranges from 830 to 950 MeV. For the purpose of comparison, we recall that the energy per baryon in ^{56}Fe amounts $M(^{56}\text{Fe})c^2/56 = 930.4$ MeV, where $M(^{56}\text{Fe})$ is the mass of the ^{56}Fe atom. Thus, with exception of the 950 MeV contour, all these curves correspond to strange matter that is *absolutely* stable, at zero external pressure, with respect to ^{56}Fe . For a representative mass of the strange quark, $m_s = 150$ MeV, which was used in this work together with $m_s = 0$, this is the case for bag constants

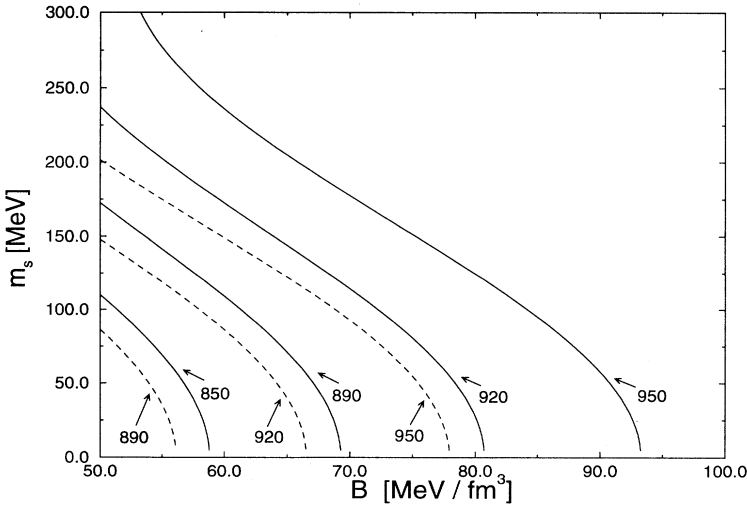


FIG. 2. Same as Fig. 1, but for a finite external bag pressure of $50 \text{ MeV}/\text{fm}^3$.

smaller than $75 \text{ MeV}/\text{fm}^3$ ($B^{1/4} = 155 \text{ MeV}$). The lower bound on B , given by $57 \text{ MeV}/\text{fm}^3$ ($B^{1/4} = 145 \text{ MeV}$), is determined by the fact that the energy per baryon number of 2-flavor quark matter must be higher than the one of ^{56}Fe . Otherwise, ^{56}Fe would be made up of u and d quarks rather than nucleons. This condition also determines the termination points of these contours, which are located at those points where the contours cross the vertical line at $B = 57 \text{ MeV}/\text{fm}^3$ [3]. Finite temperatures [like finite quark masses, or external pressures, cf. Eq. (2.31)] increase both the energy density ϵ of the bag as well as the baryon number density n_A . The impact of these increases is such that the energy contours are shifted toward smaller bag constants. This shift in B , as can be seen in Figs. 1 and 2, is quite large and amounts $\sim 20\%$, depending on the mass of the strange quark. The impact of finite external bag pressures, p , on the energy contours is illustrated in Fig. 2. A comparison with Fig. 1 shows that the energy contours are shifted toward smaller B values, too, which can be understood mathematically by means of combining Eqs. (2.22) and (2.24) to $B = (n_A E_A - 3p)/4$. [In the case of finite temperatures, or masses, the corresponding relation is obtained from Eq. (2.36).] From the physical point of view, this becomes clear by remembering that finite p values increase the pressure which acts on the bag from the outside, Eq. (2.1). So B can be reduced on the account of p .

The relative quark and lepton composition of quark-star matter at zero temperature is shown in Fig. 3. All quark flavor states that become populated in such matter up to densities of $10^{19} \text{ g}/\text{cm}^3$ are taken into account. Since the Coulomb interaction is so much stronger than the gravitational, quark-star matter must be charge neu-

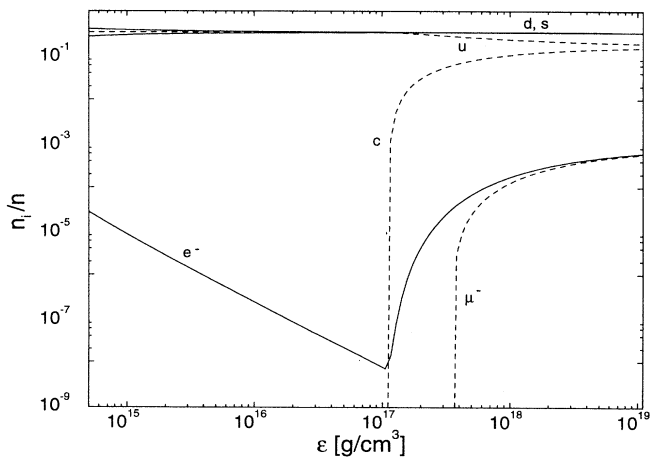


FIG. 3. Relative densities of quarks ($q = u, d, c, s$) and leptons ($l = e^-, \mu^-$), n_i/n , where $n \equiv \sum_{i=q,l} n_i$, in cold, β -stable, electrically charge neutral quark-star matter as a function of energy density. (Here and in all subsequent calculations a bag constant of $B^{1/4} = 145 \text{ MeV}$ has been chosen.)

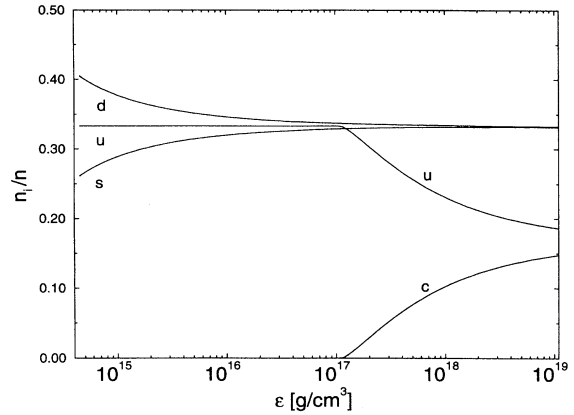


FIG. 4. Enlargement of the upper portion of Fig. 3.

tral to very high precision [8]. Therefore, any net positive quark charge must be balanced by a sufficiently large number of negatively charged quarks and leptons present in the system, as shown in Fig. 3. An enlargement of the upper portion of this figure is exhibited in Fig. 4. One sees that at lower densities the number of d quarks is somewhat larger than that of s quarks, due to the finite mass of the strange quarks. The behavior of n_d/n and n_s/n can be understood qualitatively from Eq. (2.25), which reveals that $n_d/n_s = (1 - m_s/\mu_s)^{-3/2}$. Since $m_s/\mu_s < 1$ it follows that $n_d > n_s$ at all densities, and, secondly, $n_d \xrightarrow{\epsilon \rightarrow \infty} n_s$ from above since $m_s/\mu_s \xrightarrow{\epsilon \rightarrow \infty} 0$ (cf. Fig. 9). (Strange and charm quark masses of respectively 0.15 GeV and 1.2 GeV are assumed.) In contrast with the sensitive density dependence of lepton number, the abundances of u , d , and s quarks in strange matter vary only rather weakly with density. The situation is different for the c quarks whose concentration increases at threshold density extremely rapidly. At still higher densities it tends against the concentration of u quarks, and charge neutrality is nearly achieved by appropriate concentrations of quarks of both charge states only. The slight deficit of negative quark charge is delivered to the system by electrons and muons, whose concentrations increase monotonically for all densities larger than the threshold density of the positively charged c quarks.

C. Quark matter at finite temperature

To derive the equation of state of quark-star matter at finite temperature, up to about $T \sim 50 \text{ MeV}$, we perform a perturbation expansion of pressure $p_i = p_i(\mu, x, T)$ and baryon density $n_i = n_i(\mu, x, T)$ about their zero-temperature values, $p_{i,0} \equiv p_i(\mu_0, x_0, T_0)$ and $n_{i,0} \equiv n_i(\mu_0, x_0, T_0)$, where $T_0 = 0$ [25]. By means of writing these functions in the form $\chi_i(\mu, x, T) \equiv \chi_i(\mu_0 - \Delta\mu, x_0 + \Delta x, T_0 + \Delta T)$, where χ_i stands for p_i and n_i , expanding them in a Taylor series and keeping only the lowest order terms, one obtains

$$\chi_i(\mu, x, T) \approx \chi_{i,0} + \left. \frac{\partial \chi_i}{\partial \frac{\Delta \mu}{\mu_0}} \right|_{\mu_0, x_0, T_0} \frac{\Delta \mu}{\mu_0} + \left. \frac{\partial \chi_i}{\partial \Delta x} \right|_{\mu_0, x_0, T_0} \Delta x + \left. \frac{\partial \chi_i}{\partial \frac{T^2}{\mu_0^2}} \right|_{\mu_0, x_0, T_0} \frac{T^2}{\mu_0^2}, \quad (2.33)$$

with $\chi_{i,0} \equiv \chi_i(\mu_0, x_0, T_0)$. Above, the definitions $\Delta \mu \equiv \mu_0 - \mu$ and $\Delta x \equiv x - x_0$ have been introduced, where $\mu_0 \equiv \mu(T_0)$ and $x_0 \equiv x(T_0)$. The major problem encountered now consists in calculating the expansion coefficients occurring in Eq. (2.33), $\partial \chi_i / \partial (\Delta \mu / \mu_0)$, $\partial \chi_i / \partial \Delta x$, and $\partial \chi_i / \partial (T / \mu_0)^2$. Their determination is outlined in detail in the Appendix. It should be noticed that since

$\partial \chi_i / \partial (T / \mu_0) = 0$, which is shown in Ref. [31], both pressure and particle density depend in lowest-order only quadratically on temperature. After considerable algebra one arrives for pressure, particle density, and total energy density at the relations (the quantities a and b are defined in the Appendix)

$$p_i = p_{i,0} + \frac{1}{6} g_i T^2 \mu_0^2 \left[-a \eta_i^4 (1 - z_i^2)^{\frac{3}{2}} + b c_i \eta_i^3 (1 - z_i^2)^{\frac{3}{2}} + \frac{1}{2} \eta_i^2 \left(1 - \frac{1}{2} z_i^2 \right) \right], \quad (2.34)$$

$$n_i = n_{i,0} + \frac{1}{2} g_i T^2 \mu_0 \left[-a \eta_i^3 \sqrt{1 - z_i^2} + b c_i \eta_i^2 \sqrt{1 - z_i^2} + \frac{1}{3} \eta_i \right], \quad (2.35)$$

$$\epsilon = 3p + 4B + \sum_{i=s,c,\mu^-} \frac{g_i \mu_0^2 \eta_i^2}{2} \left(\frac{\mu_0^2 \eta_i^2}{2\pi^2} z_i^2 \left(\sqrt{1 - z_i^2} - z_i^2 \ln \frac{1 + \sqrt{1 - z_i^2}}{z_i} \right) + T^2 \left(z_i^2 \sqrt{1 - z_i^2} (b c_i \eta_i - a \eta_i^2) + \frac{1}{6} z_i^2 \right) \right), \quad (2.36)$$

with the definition

$$c_i \equiv \begin{cases} +1 & \text{if } i = e^-, \mu^-, \\ 0 & \text{if } i = d, s, \\ -1 & \text{if } i = u, c. \end{cases} \quad (2.37)$$

The comparison of these relations with the corresponding ones obtained for zero-temperature and massless quarks, derived in Sec. II A, immediately reveals the impact of finite temperatures and masses on the equation of state. Notice that in the limit of $T \rightarrow 0$, the zero-temperature equation of state (2.31) is obtained from Eq. (2.36). Furthermore, as outlined just above, the temperature depen-

dence in the lowest-order expansion enters only quadratically in T .

The equation of state of strange matter at nonzero temperature, computed for Eq. (2.36), is shown in Fig. 5. There is a noticeable influence of temperature on the equation of state only near the saturation density of $\epsilon \sim 4B$, as can be seen from Fig. 6.

The expressions for particle density and pressure of electrons are given by [recall that $x(T) \equiv \mu_{e^-}(T) / \mu(T)$, which reads at zero temperature $x_0 \equiv \mu_{e^-,0} / \mu_0$]

$$n_{e^-} = \frac{\mu_0^3 x_0^3}{3\pi^2} + T^2 \mu_0 \left[-a x_0^3 + b x_0^2 + \frac{1}{3} x_0 \right], \quad (2.38)$$

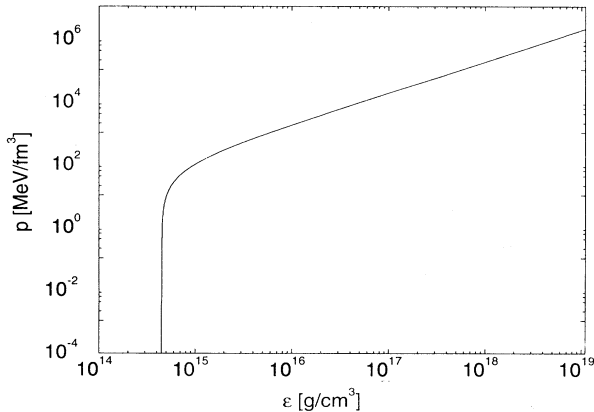


FIG. 5. Pressure isotherm versus mass density of electrically charged neutral quark-star matter. The impact of temperatures $T \leq 50$ MeV, which is significant at low nuclear densities only, is exhibited in Fig. 6.

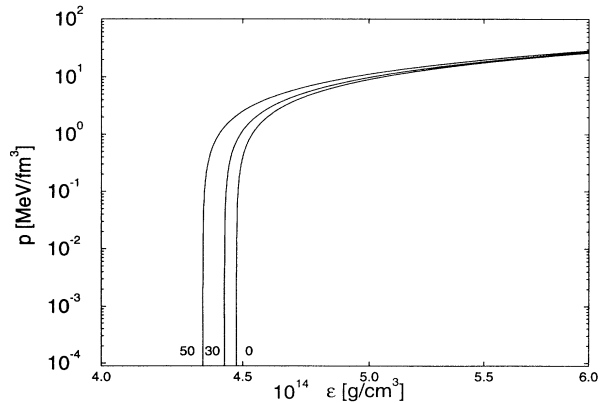


FIG. 6. Enlargement of the left portion of Fig. 5. The numbers associated to these pressure isotherms refer to temperature (in MeV). The value of the bag constant (here and for all other calculations) is $B = 1 \times 10^{14} \text{ g/cm}^3 (= 57 \text{ MeV/fm}^3)$.

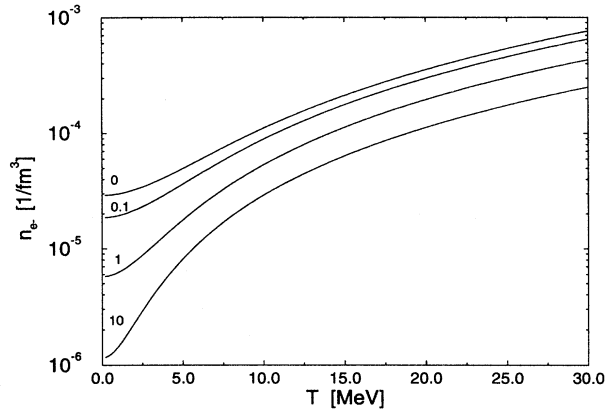


FIG. 7. Density isobars of electrons, n_{e^-} , versus temperature for different external pressure values, $p/(10^{15} \text{ g/cm}^3) = 0, 0.1, 1, 10$, which are constant along each curve. (Dividing the pressure expressed in units of g/cm^3 by 1.78×10^{12} leads to pressure in units of MeV/fm^3 .)

$$p_{e^-} = \frac{\mu_0^4 x_0^4}{12\pi^2} + \frac{1}{3} T^2 \mu_0^2 \left[-ax_0^4 + bx_0^3 + \frac{1}{2}x_0^2 \right], \quad (2.39)$$

which follow from Eqs. (2.34) and (2.35) applied to (massless) electrons, rather than massive quarks [$\eta_{e^-} = x_0$, $z_{e^-} = 0$, $c_{e^-} = 1$, according to Eqs. (2.17), (2.18), and (2.37)]. The temperature dependence of n_{e^-} for zero and finite external bag pressures, p , is exhibited in Fig. 7. Because finite p values increase the system's total energy density [cf. Eq. (2.36)], fewer electrons are necessary in order to achieve electric charge neutrality and therefore the n_{e^-} isobars move downward with increasing pressures. Temperatures, typical for newly formed massive stars, increase n_{e^-} by roughly two orders of magnitude, depending on external pressure. The quadratic dependence of n_{e^-} on T , Eq. (2.38), is significant at lower temperatures. For larger T , the implicit temperature dependence of the expression in square brackets weakens

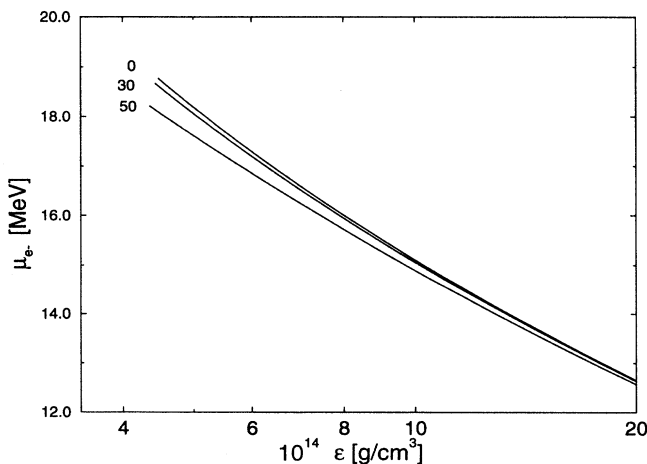


FIG. 8. Chemical potential of electrons, μ_{e^-} , versus energy density in electrically charged neutral quark-star matter at temperatures $T = 0, 30$, and 50 MeV , which are constant along these curves.

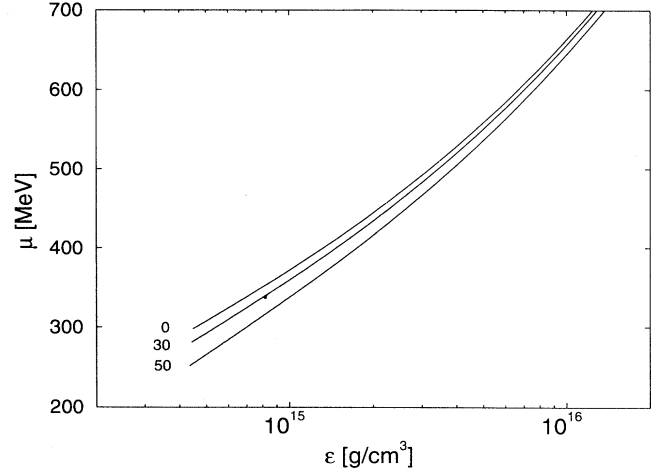


FIG. 9. Same as Fig. 8, but for the chemical potential, μ ($= \mu_d = \mu_s$), of d and s quarks [cf. Eq. (2.16)].

the increase of n_{e^-} with temperature. The variation of electron chemical potential, μ_{e^-} , along the n_{e^-} isotherms is shown in Fig. 8. One sees that μ_{e^-} deviates for temperatures $T \leq 50 \text{ MeV}$ from its zero-temperature value by at most 1 MeV ($\epsilon \sim 4B$). The decrease of μ_{e^-} with density reflects the fact that fewer electrons are needed in strange-quark matter at higher densities (cf. Fig. 3). Furthermore, we notice the downward shift of the μ_{e^-} isotherms, for a fixed density, with increasing temperature, which is due to the momentum tail of the Fermi-Dirac distribution function for $T > 0$.

The density and temperature dependence of the chemical potential of d and s quarks, μ , is graphically depicted in Fig. 9. The density dependence can be inferred qualitatively from Eq. (2.25), from which one gets $\mu = m_s(1 - n_s/n_d)^{-2/3}$. Slightly below the threshold density of s quarks one has $n_s = 0$, and therefore $\mu_s = m_s$ there. The other extreme, high s quark densities, is characterized by $n_s \rightarrow n_d$, as is known from Figs. 3 and 4. This implies that μ becomes very large in the high-density regime. In Sec. III it will be shown that stable strange stars possess central densities of at most $\sim 2 \times 10^{15} \text{ g/cm}^3$. Therefore, from Fig. 9, μ never exceeds $\sim 500 \text{ MeV}$ in such stars. This value is considerably smaller than the mass of the charm quark. Concerning the impact of temperature on μ , it is most significant at densities $\epsilon \sim 4B$ for the same reasons as already outlined in connection with the discussion of Figs. 5 and 6. Finally, finite temperatures reduce μ below its zero-temperature value. The reason is, again, the occurrence of the Fermi-Dirac function in Eq. (2.6) instead of the step function, leading to smaller chemical potentials for a fixed density. For the selected temperatures, this reduction amounts at most $\sim 100 \text{ MeV}$.

III. HYDROSTATIC EQUILIBRIUM SEQUENCES OF QUARK MATTER STARS

The masses of the two families of quark-matter stars, strange and charm ones, as a function of central density,

are shown in Fig. 10. The family of charm stars begins at a density of about 10^{17} g/cm³ and ends at 4×10^{18} g/cm³. It should be noticed that such dense hydrostatic equilibrium configurations also exist in the neutron star sequence at densities above that of the maximum-mass neutron star [32,33]. One of the most significant differences between both species of stars concerns the existence of a minimum-mass configuration in the neutron star sequence, $\sim 0.1 M_{\odot}$ [34]. In sharp contrast to this, the sequence of bare strange stars (no nuclear crusts), being bound primarily by the strong interaction rather than the gravitational force (gravity makes them only denser), does not possess a minimum-mass star. In fact, strange-matter objects can exist with baryon numbers in the enormous range of $10^2 \lesssim A \lesssim 10^{57}$ [3,35]. The lower bound is determined by finite size effects, and the upper one is set by the gravitational interaction, which increases with A , and therefore makes strange stars possessing too large central densities unstable against gravitational collapse (cf. Sec. V). (The situation is the same as for the purely gravitationally bound neutron stars.)

Temperatures typical for newly formed pulsars influence the bulk properties of quark stars, such as mass and radius, only rather weakly, as can be seen from Figs. 10 and 11. Shown are star sequences that are obtained as solutions of the Oppenheimer-Volkoff equations [36], thus being in hydrostatic equilibrium. As is well known [32], hydrostatic equilibrium alone does not guarantee stability of a compact star. The still missing ingredient is a stability analysis against radial oscillations (acoustical modes), which will be performed in Sec. V. There it will turn out that the charm-star sequence is unstable against radial oscillations. Thus we are left with the possible existence of strange-quark stars only.

The mass-radius relationship of the quark stars of Fig.

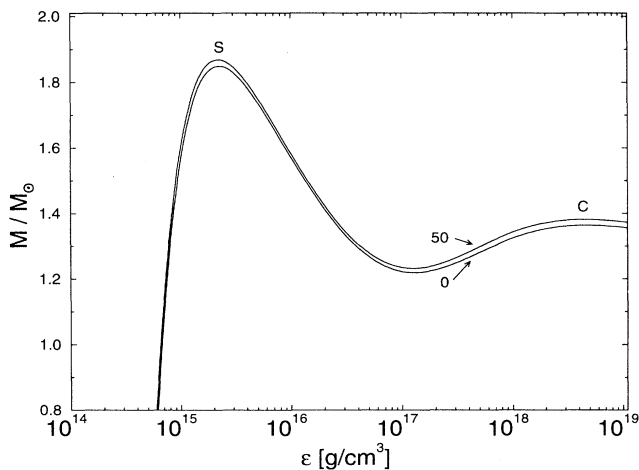


FIG. 10. Gravitational mass of quark stars (in units of solar mass) at zero and finite temperature ($T = 30$ MeV) versus central energy density. The two mass peaks labeled S and C denote the maximum-mass star of the strange- and charm-quark star sequence, respectively.

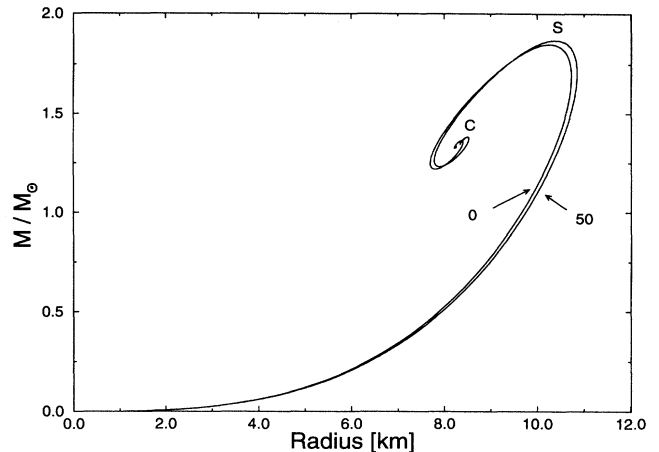


FIG. 11. Gravitational mass (in units of solar mass) versus radius of the strange- and charm-quark star sequences exhibited in Fig. 10. The symbols S and C again denote the maximum-mass model of each sequence.

10 is shown in Fig. 11. For masses larger than $\sim 0.5 M_{\odot}$ it too bears a strong similarity with the one of neutron stars. Temperatures $T \lesssim 50$ MeV modify the properties of the more massive stars of the sequence only slightly. According to above, all stars possessing central densities larger than model S are unstable against radial oscillations. The same inwardly directed spiraling behavior was also obtained for stars constructed for baryon matter equations of state that were extrapolated to the super-high density regime [32], which shows again that this behavior is not specific to self-bound stars but rather manifests the dominant role of gravity at such high densities.

IV. ELECTRONS IN STRANGE STARS

As shown in Sec. II, because the strange-quark mass is larger than that of the u and d quarks, equilibrium strange matter contains an approximately equal mixture of all three, with a slight deficit of s quarks. A relatively small number of electrons is necessary to make the system electrically charge neutral. The electrons, being bound to the system by the electromagnetic interaction and not by the strong force, extend several hundred fermis beyond the boundary of the strange star [14], which itself has a surface thickness of the order of the strong interaction range. Associated with this electron layer at the surface of hypothetical strange stars is a strong electric field, which is radially outwardly directed. Most importantly for the glitch behavior and probably the cooling of strange pulsars (pulsars interpreted according to Witten's hypothesis as rotating strange-matter stars) [4,17], this layer can carry a solid nuclear crust suspended out of contact with the pulsar's strange-matter core [14], which prevents the ion-quark matter reactions by which (atomic) crust matter would be converted into the true ground-state, strange matter. In the following, the be-

havior of the electrostatic potential of the electrons inside and in the close vicinity outside of strange stars is determined and, specifically, its *temperature dependence* studied. This analysis serves also to investigate, as a by-product, the temperature dependence of the Coulomb barrier, associated with the difference of the electrostatic potential at the surface of the strange core and the base of the inner nuclear crust. (This constitutes an extension to finite temperatures of the zero-temperature analysis performed in Ref. [14].)

A. Impact of finite temperatures on the electrostatic potential of electrons

1. Inside strange stars

Firstly, the electrostatic potential of electrons $V(r)$ inside a bare strange star is determined. For this purpose we recall that locally the energy of an electron sitting at the fermi surface is given by $\mathcal{E}(r) \equiv \mu_{e^-}(r) - eV(r)$ [14,25], where $\mu_{e^-}(r)$ denotes the electron's radially dependent chemical potential. In equilibrium, $d\mathcal{E}(r)/dr = 0$. From the boundary conditions $V(r) \xrightarrow{r \rightarrow \infty} 0$ and $\mu_{e^-}(r) \xrightarrow{r \rightarrow \infty} 0$ [14] it follows that $eV(r) = \mu_{e^-}(r)$ [25]. The density dependence of $\mu_{e^-}(r)$ has already been determined in Sec. II. Plotting $\mu_{e^-}(r)$ as a function of radial distance, from the star's origin to the surface, leads to Fig. 12, which exhibits the behavior of $V(r)$ inside of strange stars with representative gravitational masses and temperatures. Since μ_{e^-} decreases with density, Fig. 8, the electrostatic potential of electrons increases mono-

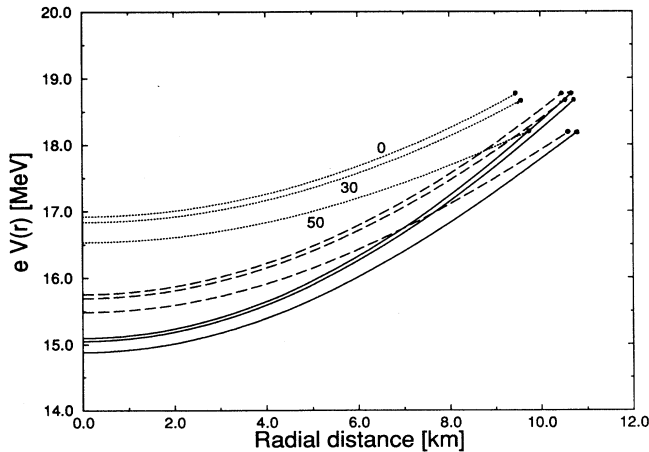


FIG. 12. Electrostatic potential, $eV(r)$, of electrons inside ($r < R$) strange stars of masses $M/M_\odot = 1$ (dotted curves), 1.4 (dashed), and 1.6 (solid). The temperatures in each case are $T = 0, 30$, and 50 MeV. Notice that the termination points of these curves, marked with solid dots, actually lie several hundred fermi inside of R (see Fig. 13).

tonically from the center toward the surface of strange stars. Finite temperatures influence the $eV(r)$ isotherms more significantly in the vicinity of the surface of strange stars than at their centers because the density is smallest there. For the heavier stars, which possess larger central densities, the isotherms are shifted downward, which is a consequence of the decreasing behavior of μ_{e^-} with density (Fig. 8). Another noteworthy feature is that independent of star mass (and thus, central star density), all isotherms referring to the same temperature terminate at the *same* value of $eV(R)$. This is indicated by the solid dots, which possess the same height for the same temperature. This independence of mass, or in other words, of central star density, becomes clear from Fig. 8, which shows that the value of μ_{e^-} at the star's surface is determined only by the values of bag constant and temperature. It also explains the shifts of the termination points for increasing temperatures toward larger radii.

2. Surface region

In the second step, the behavior of $V(r)$ several hundred fermi inside and outside of the surface of a strange star is determined. For this purpose we recall that due to the rearrangement of electron charge there, the net positive charge of the quarks will be balanced *locally* by electrons only up to radial distances $r \leq R_m$ (star's bulk matter part), where R_m is only slightly smaller than the star's radius, $R_m \lesssim R$. Beyond R_m , in the region $R_m \leq r \leq \infty$, the condition of electric charge neutrality is a *global* (rather than a local) one. In order to determine R_m , we note that from Poisson's equation for radii in the range $R_m < r < \infty$,

$$\frac{d^2 eV}{dr^2} = 4\pi e^2 [n_{e^-}(r) - n_q(r)] \Theta(r - R_m) \quad (4.1)$$

(the dV/dr term can be neglected here; $3n_q \equiv 2n_u - n_d - n_s$, $n_q - n_{e^-} = 0$ for $r < R_m$) it follows that

$$\int_{R_m}^R dr n_q(r) = \int_{R_m}^{\infty} dr n_{e^-}(r), \quad (4.2)$$

since $dV(R_m)/dr = dV(\infty)/dr = 0$. The first relation follows from the fact that $V(r)$ attains a maximum at R_m . The upper boundary in the second integral reflects the circumstance that the electrons extend beyond the surface of the strange star. Equation (4.2) can be transformed to

$$\int_{V(R_m)}^{V(R)} dV n_q = \int_{V(R_m)}^{\infty} dV n_{e^-}. \quad (4.3)$$

Using $edV = d\mu_{e^-}$ and $n_{e^-} = \partial p_{e^-} / \partial \mu_{e^-}$ [cf. Eq. (2.6)], Eq. (4.3) can be written as

$$\int_{V(R_m)}^{V(R)} dV n_q = \frac{1}{e} \int_{\mu(R_m)}^{\mu(\infty)} d\mu_{e^-} \frac{\partial p_{e^-}}{\partial \mu_{e^-}} = \frac{1}{e} [p_{e^-}(\infty) - p_{e^-}(R_m)] . \quad (4.4)$$

Because R and R_m differ only by a few hundred fermi [14], the density $n_q(r)$ in that range can be treated as being independent of r . Its value is therefore given, to a very good approximation, by $n_q(r) \simeq n_{e^-}(R_m)$. One thus obtains, from Eq. (4.4),

$$eV(R, T) = \mu_{e^-}(R_m, T) - \frac{p_{e^-}(R_m, T) - p_{e^-}(\mu_{e^-} = 0, T)}{n_{e^-}(R_m, T)} . \quad (4.5)$$

By means of the approximation $\mu_{e^-}(R_m, T) \simeq \mu_{e^-}(R, T)$ and substituting p_{e^-}/n_{e^-} with Eqs. (2.38) and (2.39), one obtains, for Eq. (4.5) (recall that the zero-temperature chemical potential of electrons, $\mu_{e^-}(T=0)$, is abbreviated $\mu_{e^-,0}$),

$$eV(R, T) \simeq \mu_{e^-}(R, T) - \frac{\mu_{e^-,0}^4(R) + 4\pi^2 T^2 \mu_0^2(R) [-ax_0^4(R) + bx_0^3(R) + \frac{1}{2}x_0^2(R)]}{4\mu_{e^-,0}^3(R) + 12\pi^2 T^2 \mu_0^2(R) [-ax_0^3(R) + bx_0^2(R) + \frac{1}{3}x_0^2(R)]} , \quad (4.6)$$

where, according to Eq. (2.18) and Eq. (A21) of the Appendix, the electron chemical potential at finite temperature is given by

$$\mu_{e^-}(R, T) \equiv \mu(R, T) x(R, T) = \left(\mu_0(R) - a\pi^2 \frac{T^2}{\mu_0} \right) \left(x_0(R) + b\pi^2 \frac{T^2}{\mu_0^2} \right) . \quad (4.7)$$

In the special case of $T=0$ one immediately obtains from Eq. (4.6) the simple relation [14]

$$eV(R, T) \Big|_{T=0} = \frac{3}{4} \mu_{e^-,0}(R) , \quad (4.8)$$

from which it follows that the electrostatic potential of electrons at the surface of the star's strange-matter core is *reduced* relative to its value obtained by imposing the condition of local (instead of global) charge neutrality [14], which, due to the rearrangement of electron charge, holds only for radii $r \leq R_m$ (cf. beginning of this section). As will be shown below (cf. Fig. 15), finite temperatures lead to an even stronger reduction of the electrostatic

electron potential, which amounts at most 50% for $T \leq 50$ MeV. From Eq. (4.6) one sees that this decrease has its origin in the reduction of μ_{e^-} with T (exhibited in Fig. 8), which is additionally strengthened by the second term on the right-hand side of this equation. As an example, the values of $\mu_{e^-}(R, T=0)$ and $eV(R, T=0)$, 18.8 and 14.1 MeV, respectively, reduce to 18.7 MeV and 9.5 MeV at $T=30$ MeV, which shows that the temperature dependence of the second term in Eq. (4.6) prevails over the one of the first term.

Lastly, we determine $V(r)$ in the regions $R_m \leq r \leq R$ and $R \leq r \leq R_{\text{crust}}$. The second region corresponds to distances that lie outside of the star's strange-matter core. Two regions there are to be distinguished. The first one extends from the core's surface, at $r=R$, to that radial distance where the inner nuclear crust (referred to henceforth as the crust's base) begins, denoted $r=R_{\text{crust}}$. The associated width, $R_{\text{gap}} \equiv R_{\text{crust}} - R$, is referred to henceforth as gap. The second region begins at R_{crust} , and extends in the radial outward direction toward infinity. The behavior of the electrostatic potential in the surface region is determined by Poisson's equation

$$\frac{d^2 eV}{dr^2} + \frac{2}{r} \frac{deV}{dr} = \frac{4\pi e^2}{3} \left\{ \left[\frac{1}{\pi^2} [(eV)^3 - (eV(R_m))^3] + T^2 [eV - eV(R_m)] \right] \Theta(r - R_m) \Theta(R - r) + \left[\frac{1}{\pi^2} (eV)^3 + T^2 eV \right] \Theta(r - R) \Theta(R_{\text{crust}} - r) \right\} . \quad (4.10)$$

Notice that in the first term on the right-hand side ($R_m < r < R$) the net charge density of electrons and quarks, $n_{e^-}(r) - n_q(r)$, enters, where $n_q(r) \simeq n_{e^-}(R_m) = [eV(R_m)]^3 / 3\pi^2$. By definition, the quark density is zero in the second region, $R \leq r \leq R_{\text{crust}}$. The expression of $n_{e^-}(r)$,

$$n_{e^-}(r) = \frac{1}{3\pi^2} \mu_{e^-}^3(r) + \frac{1}{3} \mu_{e^-}(r) T^2 = \frac{1}{3\pi^2} [eV(r)]^3 + \frac{1}{3} eV(r) T^2 , \quad (4.11)$$

is computed exactly from Eq. (2.6), treating the electrons (and positrons) as massless particles.¹ An analytical representation of $V(r)$ in the gap region can be obtained at zero temperature if the dV/dr term in Eq. (4.10) is ig-

¹The pressure of electrons and positrons can be calculated exactly also in this limit. One obtains, from Eq. (2.5),

$$p_{e^-} - r = \frac{1}{12\pi^2} \mu_{e^-}^4(r) + \frac{1}{6} \mu_{e^-}^2(r) T^2 + \frac{7\pi^2}{180} T^4 ,$$

leading for Eq. (4.5) to

$$eV(R, T) = \mu_{e^-}(R, T) - \frac{3+2\pi^2 T^2 / \mu_{e^-}^2(R, T)}{4+4\pi^2 T^2 / \mu_{e^-}^3(R, T)} .$$

nored (a good approximation), i.e.,

$$\frac{d^2 eV}{dr^2} = \frac{4e^2}{3\pi} [eV(r)]^3 \Theta(r - R) \Theta(R_{\text{crust}} - r) . \quad (4.12)$$

Its solution reads

$$eV(r) = \frac{C}{r - R + C/[eV(R)]} , \quad R \leq r \leq R_{\text{crust}} , \quad (4.13)$$

with $C \equiv \sqrt{3\pi/2}/e = 5.013 \times 10^3$ MeV fm. It leads for a given crust potential, $V(r) = V_{\text{crust}}$, to

$$\begin{aligned} R_{\text{gap}} &\equiv R_{\text{crust}} - R \\ &= C \left(\frac{1}{eV_{\text{crust}}} - \frac{1}{eV(R)} \right) . \end{aligned} \quad (4.14)$$

Notice that a given value of V_{crust} determines R_{crust} , and thus R_{gap} . It is obvious that the gap disappears if the crust potential coincides with $V(R)$, the potential's value at the surface of the strange core. In this case free ions would reach the star's strange-matter core without restraint.

3. Crust region

The electrostatic potential in the nuclear crust regime, $r \geq R_{\text{crust}}$, is constant. This follows from the fact that the forces acting on the ions there, gravitational and electric, must counterbalance each other at equilibrium. Since the gravitational force is tiny compared to the electric force in the gap, one obtains $dV/dr = 0$ which implies that the electrostatic potential is constant there, that is, $V(r) \equiv V_{\text{crust}} (= \text{const})$. For what follows, representative values of $V_{\text{crust}} = 5$ and 10 MeV have been chosen, together with zero external potential [14].

B. Gap width at finite temperature

Figures 13–15 exhibit the behavior of $eV(r)$ in the close vicinity inside and outside of R . The curves differ with respect to the temperature of the strange star and the chosen value of V_{crust} . For *very low* temperatures and an electrostatic crust potential of 5 MeV, as chosen here, a large gap of $R_{\text{gap}} \sim 800$ fm results. Larger values of V_{crust} reduce the difference of the potential at the star's surface and the inner crust, which narrows the gap. For example, a value of $eV_{\text{crust}} = 10$ MeV reduces R_{gap} to about 300 fm, as can be seen from Fig. 14. This is consistent with the finding in Ref. [14]. Most interestingly is the impact of *finite* temperatures on the gap. From Eq. (4.6) it is already known that the potential's value at the star's surface, $V(R)$, is reduced in this case. Figures 13–16 exhibit that this reduction amounts up to $\sim 50\%$ for the temperatures under consideration. The associated reduction of R_{gap} with temperature is rather strong. In fact, we find that the gap even *shrinks to zero* for plausible values of both V_{crust} and temperature that would be

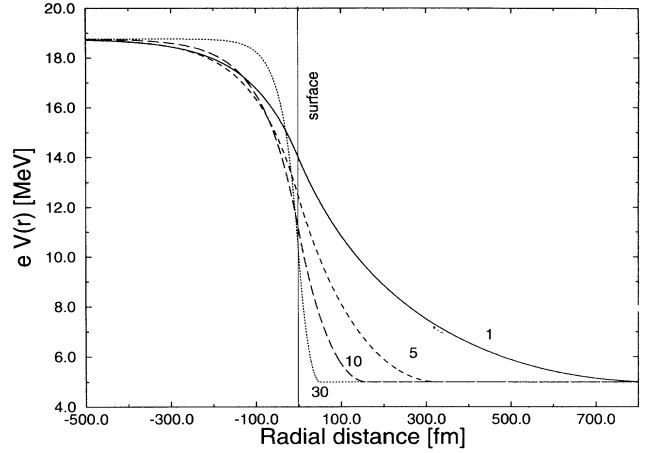


FIG. 13. Electrostatic potential of electrons in the close vicinity inside and outside of the surface of a strange star. The location of its surface is indicated by the vertical line. The figures assigned to these curves refer to temperature (in MeV). A representative value for the electrostatic crust potential, $eV_{\text{crust}} = 5$ MeV (horizontal line), which is constant (see text), has been chosen. The gap width extends from ~ 40 fm to about 800 fm, depending on temperature.

typical for newly formed strange pulsars in supernovae.

In Ref. [14], a minimum value of ~ 200 fm was established as the lower bound on R_{gap} necessary to guarantee the crust's security against strong interactions with the star's strange-matter core. Via Fig. 16 we find that a hot strange pulsar with $T = 30$ MeV cannot carry a nuclear crust whose electrostatic potential at the base is larger than $eV_{\text{crust}} \sim 0.1$ MeV. A somewhat cooler star of $T \sim 10$ MeV can carry only crusts with $eV_{\text{crust}} \lesssim 4$ MeV. Finally, crust potentials in the range 8–12 MeV

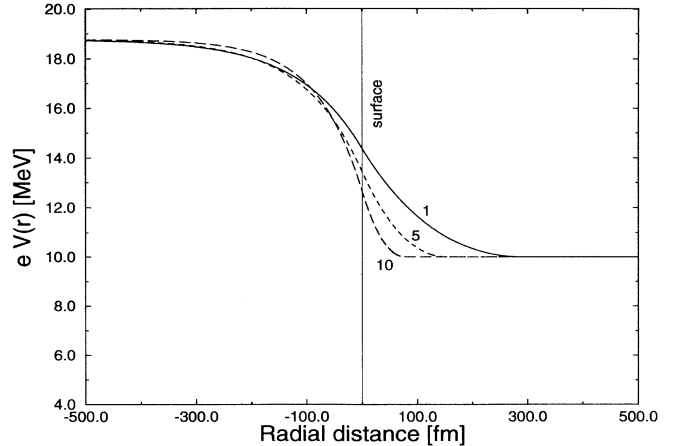


FIG. 14. Same as Fig. 13, but for a electrostatic crust potential of 10 MeV.

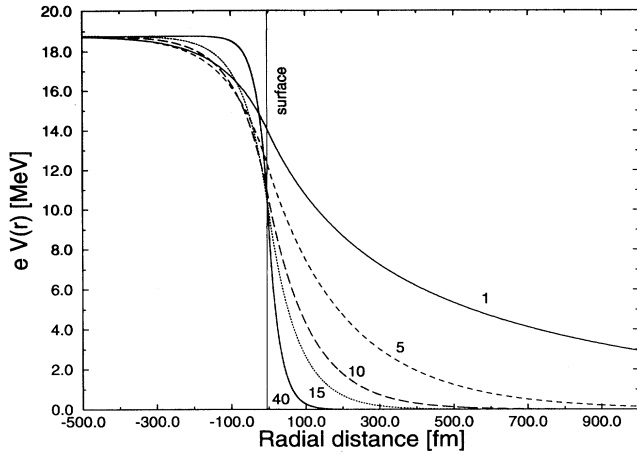


FIG. 15. Same as Fig. 13, but for zero external electrostatic potential. The labels refer to temperature (in MeV).

are possible for stars with temperatures $T \lesssim 5$ MeV. In this connection it is interesting to recall that the upper limit on the density of the inner crust is determined by neutron drip, which occurs at about 4.3×10^{11} g/cm³, where free neutrons begin to drip out of the most stable nucleus, ¹¹⁸Kr ($Z = 36$), at that density [14]. Being electrically charge neutral, the neutrons can gravitate toward the star's strange-matter core where they are converted into strange matter. The electrostatic potential in matter at such densities lies right in the above given range, ~ 10 MeV. Hence, we conclude that the constraint $V_{\text{crust}} \lesssim 10$ MeV established here provides another independent limit (in addition to the one set by neutron drip) on the maximum density of the nuclear crust that can be carried by a strange star. Accidentally, both sources lead to the same density limit. Applied to the formation of a crust on the

TABLE I. Kinetic energy, E_p , acquired by a proton falling toward the surface of a bare strange star, for a few selected strange star masses.

M/M_\odot	0.1	0.5	1.0	1.4	1.85
E_p [MeV]	36	95	187	252	350

surface of a bare strange pulsar formed in a supernova explosion, we are left with the important conclusion that its crust must be at rather low density in order to ensure a sufficiently large enough gap. In terms of mass, the crust will be much lighter than $\sim 10^{-5} M_\odot$ established for a strange pulsar possessing a nuclear crust whose density at the base is equal to neutron drip [14,37].

As a further interesting aspect, the findings presented above permit a few simple considerations concerning the accretion of matter onto the surface of a bare strange star being bound in a binary system, whose companion star is made up of ordinary matter. Furthermore, since the universe is a rather dirty environment, it seems plausible to assume that there might be strange stars that accrete some ambient (interstellar) material [14]. The idealized case of spherical accretion of a plasma, which consists of only protons and electrons, onto the surface of a bare, nonmagnetized strange star (assuming no dissipation in the radiation flow of the infalling matter) has been considered in Ref. [16]. There, it was estimated that under these circumstances, the kinetic energy of protons hitting the surface of a bare strange star is given by

$$E_p = \frac{138 M/M_\odot}{R_6 \sqrt{1 - 0.295 M/(M_\odot R_6)}} \text{ MeV}, \quad (4.15)$$

where $R_6 = R/10^6$ cm and M/M_\odot is the star's mass in units of solar mass. Via Eq. (4.15) we estimate from our results (Fig. 11) that $E_p \lesssim 250$ MeV for a strange star

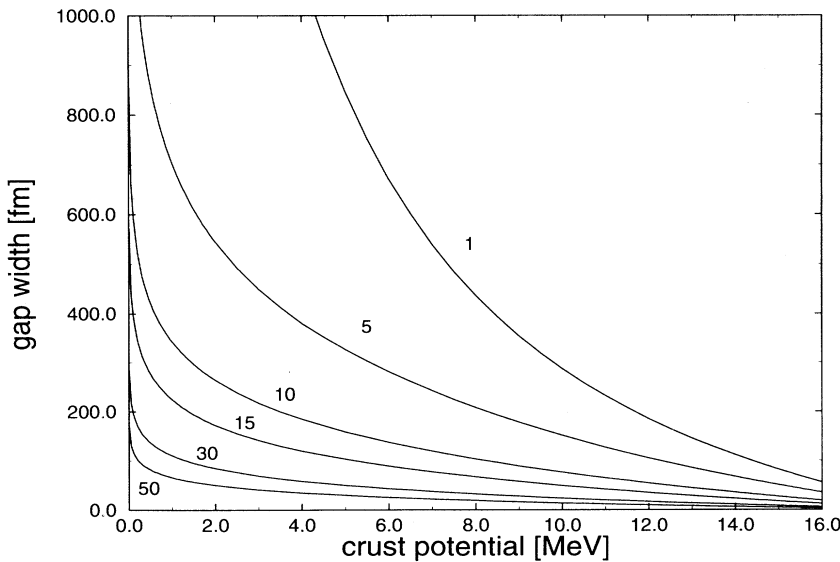


FIG. 16. Gap width R_{gap} versus electrostatic crust potential, eV_{crust} . The labels refer to temperature (in MeV).

possessing a typical pulsar mass. Further values are listed in Table I. Such high energies would enable a proton to easily penetrate the maximum possible Coulomb barrier, which has a height of $e\Delta V \sim 15$ MeV, and to undergo a reaction with the star's strange-matter core. [The barrier is defined as $e\Delta V \equiv Z(eV(R, T) - eV_{\text{crust}})$, $Z = 1$ for protons.]

V. STABILITY AGAINST RADIAL OSCILLATIONS

Below we give the equations that are to be solved to obtain the eigenfrequencies and eigenfunctions of radial normal modes of a massive star. The analysis is carried out on the basis of Einstein's field equations for a metric of the form [32,38]

$$ds^2 = e^{2\nu(r)} dt^2 - e^{2\lambda(r)} dr^2 - r^2 (d\theta^2 + \sin^2\theta d\phi^2). \quad (5.1)$$

The adiabatic motion of the star in its n th normal mode ($n = 0$ is the fundamental mode) is expressed in terms of an amplitude $u_n(r)$ by

$$\delta r(r, t) = e^{\nu(r)} u_n(r) e^{i\omega_n t} / r^2, \quad (5.2)$$

where $\delta r(r, t)$ denotes small perturbations in r . The quantity ω_n is the star's oscillation frequency, which we want to compute. The eigenequation for $u_n(r)$, which governs the normal modes, has the Sturm-Liouville form

$$\frac{d}{dr} \left(\Pi(r) \frac{du_n(r)}{dr} \right) + [Q(r) + \omega_n^2 W(r)] u_n(r) = 0. \quad (5.3)$$

The functions $\Pi(r)$, $Q(r)$, and $W(r)$ are expressed in terms of the equilibrium configurations of the star by

$$\Pi = e^{(\lambda+3\nu)} r^{-2} \Gamma P, \quad (5.4)$$

$$Q = -4e^{(\lambda+3\nu)} r^{-3} \frac{dP}{dr} - 8\pi e^{3(\lambda+\nu)} r^{-2} P (\epsilon + P) + e^{(\lambda+3\nu)} r^{-2} (\epsilon + P)^{-1} \left(\frac{dP}{dr} \right)^2, \quad (5.5)$$

$$W = e^{(3\lambda+\nu)} r^{-2} (\epsilon + P). \quad (5.6)$$

The quantities ϵ and P in Eqs. (5.4)–(5.6) denote the energy density (total mass energy) and the pressure of the stellar equilibrium configuration as measured by a local observer. The pressure gradient dP/dr is obtained from the Oppenheimer-Volkoff equations. The symbol Γ denotes the varying adiabatic index at constant entropy, given by

$$\Gamma = \frac{(\epsilon + P)}{P} \frac{\partial P}{\partial \epsilon}. \quad (5.7)$$

The boundary conditions for Eq. (5.3) are

$$u_n \sim r^3 \quad \text{at star's origin, } r = 0, \quad (5.8)$$

$$\frac{du_n}{dr} = 0 \quad \text{at star's surface, } r = R. \quad (5.9)$$

Solving Eq. (5.3) subject to the boundary conditions (5.8) and (5.9) leads to the frequency spectrum ω_n^2 ($n = 0, 1, 2, \dots$) of the normal radial modes of a given stellar model. As a characteristic feature, the eigenfrequencies ω_n^2 form an infinite discrete sequence, i.e., $\omega_n^2 < \omega_{n+1}^2$.

The four lowest-lying eigenfrequencies of quark stars are shown in Fig. 17. A comparison with their mass-central density relationship, Fig. 10, shows that these equilibrium configurations possess a characteristic mode of vibration of zero frequency ($\omega_n^2 = 0$) when and only when the star's mass attains an extremum (critical point associated with an inflection point of mass), in agreement with the theorem of Harrison and Wheeler [32]. What is not known from the theorem, however, is *which* mode is possessing a zero point. Of course it must be the lowest-lying one which was previously stable, i.e., for which $0 < \omega_n^2$. We find that it is the $n = 0$ mode which becomes zero first at a density which corresponds to the maximum-mass *strange* quark star labeled *S* in Figs. 10 and 11. Since ω_0^2 remains negative at all densities larger than this one, it follows that no quark matter stars can exist in nature that are more compact than the hypothetical strange stars. Specifically, this rules out the possible existence of *charm* stars. In fact, as one sees from Fig. 17, going to higher and higher central star densities leads to the successive excitation of more and more unstable modes, i.e., $\omega_n^2 < 0$ with $n = 1, 2, 3, \dots$, and thus no quark stars more massive than strange stars satisfy the condition $\omega_n^2 > 0$ for *all* $n \geq 0$, which is necessary for stability. This situation is analogous to that of hydrostatic equilibrium configurations in the neutron star sequence with central densities above that of the maximum-mass

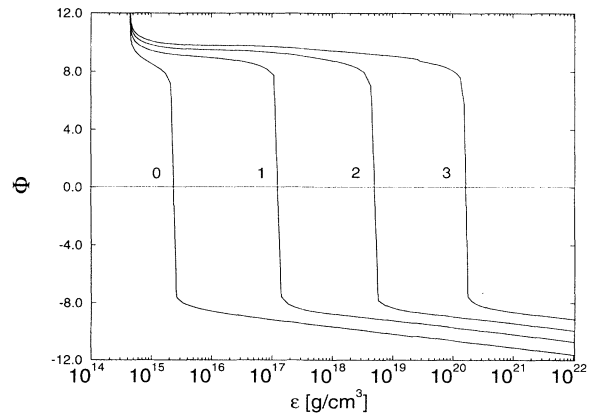


FIG. 17. Pulsation frequencies of the lowest four ($n = 0, 1, 2$, and 3) normal radial modes of quark matter stars as a function of central star density. For convenience, on the y axis the quantity $\Phi(a) \equiv \text{sgn}(a) \log_{10} [1 + \text{abs}(a)]$ with $a \equiv (\omega_n/\text{sec}^{-1})^2$ is plotted instead of ω_n^2 itself.

TABLE II. Periods of radial oscillation, τ_n , of a few selected strange-star models.

M/M_\odot	10^{-3}	10^{-2}	0.1	0.5	1.0	1.4	1.6	1.85
τ_0 [ms]	0.0123	0.0270	0.0614	0.125	0.197	0.279	0.353	∞
τ_1 [ms]	6.165×10^{-3}	0.0134	0.0301	0.0581	0.084	0.106	0.121	0.160
τ_2 [ms]	4.11×10^{-3}	0.895×10^{-3}	0.0200	0.0382	0.055	0.068	0.0769	0.0974

neutron star.

Finally, we point out that the instability of the charm stars is already indicated by the small values of the adiabatic index Γ , defined in Eq. (5.7), of a ultrarelativistic quark gas [15]. By means of Eq. (2.22) and Figs. 5 and 10 one sees that $\Gamma \approx 4/3$ at charm-star densities. Stability of a stellar model with respect to small radial perturbations in the *post-Newtonian approximation* requires that $\Gamma > 4/3 + 2M\kappa/R$, where $\kappa \sim 1$ [39]. For typical masses and radii of charm stars, $\sim 1.3 M_\odot$ and ~ 8 km respectively (see Figs. 10 and 11), one finds $2M\kappa/R \sim 0.5$, leading to $\Gamma \gtrsim 5/3$ for such stars. Therefore, the less deeply analysis of the adiabatic index, performed in the post-Newtonian approximation, indicates that the family of charm stars may be unstable against radial oscillations. (Of course, from this simplified analysis alone one cannot definitely conclude that charm stars are unstable.)

Figure 18 exhibits the oscillation amplitudes of the first few vibrational modes of a strange-quark star with mass $M \sim 0.5 M_\odot$. One sees that the number of nodes associated with an oscillation is equal to its order, n , as determined by the mathematical structure of the eigenvalue equation. Specifically, the $n = 0$ mode of oscillation is free of nodes. The corresponding periods of radial oscillation, $\tau_n \equiv 2\pi/\omega_n$, whose values are listed in the figure caption, lie in the millisecond range, which is consistent with the findings of Ref. [40]. Table II shows that

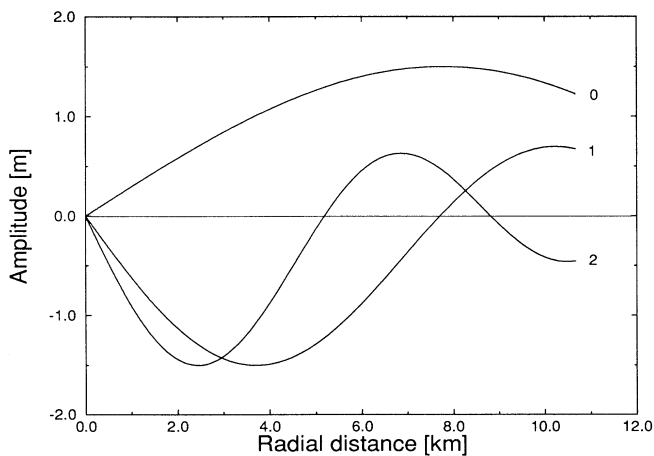


FIG. 18. Amplitudes of the three lowest-lying eigenmodes of oscillation ($n = 0, 1, 2$) of a strange star possessing a representative mass of $M \sim 1.5 M_\odot$. The associated periods of radial oscillation are $\tau_0 = 0.334$ ms, $\tau_1 = 0.117$ ms, and $\tau_2 = 0.075$ ms.

the lighter the strange star, the smaller the oscillation periods. Indeed, in the limit of vanishing star masses, which are obtained for $\epsilon \rightarrow 4B$, the periods of all modes of strange stars go to zero, as shown in [41]. This behavior arises because $\Gamma \rightarrow \infty$ when $\epsilon \rightarrow 4B$, that is, $p \rightarrow 0$, when the central density of the strange star tends toward its smallest possible value [15]. As known from Fig. 17, the frequency of the fundamental mode, ω_0 , of the most massive strange star (labeled *S* in Fig. 10) is zero. Therefore, $\tau_0 = \infty$ for that star model. The higher acoustical modes of vibration of the maximum-mass star are nonzero. They pass through zero at higher densities (Fig. 17).

The impact of finite temperatures on the periods of the fundamental radial oscillation, τ_0 , of light strange stars is illustrated in Fig. 19. It is significant only for stars with masses $M \lesssim 1 M_\odot$ (cf. Fig. 10), whose properties are most sensitive against variations of temperature. It is interesting to compare these periods with those of neutron stars, which reveals that the oscillation periods of neutron stars, constructed for a few selected nuclear equations of state [41], attain a minimum value of $\tau_0 \sim (0.3 - 0.4)$ msec at intermediate star masses. This is different for strange stars, due to their different generic mass-radius relationship, for which τ_0 is smaller, the lighter the star (cf. Table II). Both types of stars with masses $M \gtrsim 1 M_\odot$ seem to possess periods of oscillation of the same magnitude.

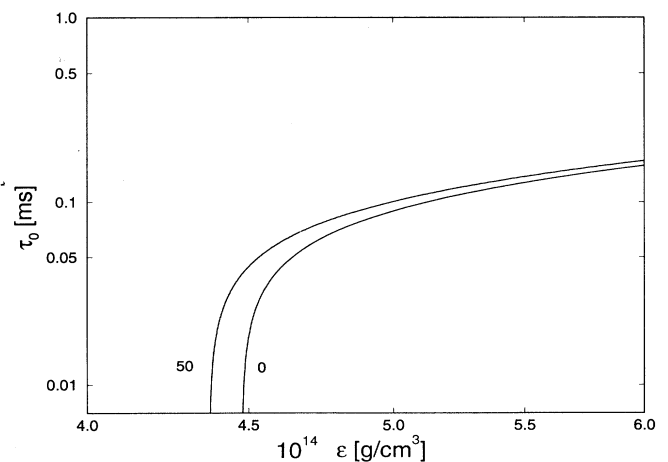


FIG. 19. Lowest-lying periods of radial oscillation, τ_0 , of strange stars versus central star density, for star temperatures $T = 0$ and 50 MeV.

VI. SUMMARY

The purpose of this work consists in a detailed investigation of the structure and stability of strange and charm stars at finite temperatures. It is found that temperatures $T \leq 50$ MeV modify the equation of state significantly only at energy densities that are close to $\sim 4B$, i.e., at small external bag pressures. The situation is different for the electrons since they are bound to the system by the electromagnetic interaction rather than the strong force, as is the case for the quarks. Correspondingly, the electron density varies for temperatures in the range $0 \leq T \leq 50$ MeV between one and two orders of magnitude. A change of the density of electrons is accompanied by a change of their chemical potential, which, however, is smaller than $\lesssim 1$ MeV. As a consequence of the weak temperature dependence of the equation of state, the bulk properties of sequences of strange stars also exhibit only a weak dependence on temperature. The quark/lepton composition of quark-star matter is determined up to those densities at which even charm-quark states become populated. We find that this takes place at densities slightly larger than 10^{17} g/cm³. In order to fulfill the condition of electric charge neutrality, there is only a slight need for electrons. Muons are completely absent in strange-star matter, and become populated only at densities larger than the threshold density of charm quarks.

Of crucial importance for the existence of nuclear crusts on the surfaces of bare strange stars is the existence of a Coulomb barrier associated with the difference of the electrostatic potential at the surface and the base of the crust. It is found that finite temperatures lead to a considerable reduction of the Coulomb barrier, which favors the tunneling of ions (atomic nuclei) bound in the nuclear crust toward the strange star surface. In fact, the electrostatic potentials at the surface of a hot strange star and at the base of its inner crust may even become equal at temperatures that are typical for newly formed pulsars, $T \sim (30 - 50)$ MeV. Thus, the Coulomb barrier, which prevents the ions in the crust from coming into contact with the star's strange matter core, disappears and consequently conversion of confined baryonic matter into strange matter is not prohibited any longer. Therefore, we conclude that hot strange stars are unlikely to possess nuclear crusts as long as their temperatures are larger than about 5 MeV, depending on the value of the crust's electrostatic potential at its base.

Another important topic of this article consists in performing a stability analysis of quark-matter stars against radial oscillations. It is found that the fundamental eigenmode passes through zero at the density of the most massive strange star. It is positive at all densities smaller than this one. Thus, strange stars are stable against radial oscillations. The situation is different for all quark stars having central densities larger than the maximum-mass strange star. For all such configurations the fundamental mode is found to be unstable. More than that, going to higher and higher central star density leads to the successive excitation of higher-lying eigenmodes. We thus arrive at the very important conclusion that no

quark-matter stars can exist in nature other than the hypothetical strange stars. Specifically, this rules out the possible existence of charm-quark stars.

ACKNOWLEDGMENTS

This work was supported by the Director, Office of Energy Research, Office of High Energy, and Nuclear Physics, Division of Nuclear Physics, of the U.S. Department of Energy under Contract DE-AC03-76SF00098. We appreciate discussions with Ch. Alcock and J. Madsen.

APPENDIX: FINITE-TEMPERATURE EXPANSION

The coefficients occurring in the expansion of pressure, Eq. (2.33), are obtained from Eqs. (2.5) and (2.6) as

$$\frac{\partial p_i}{\partial \frac{\Delta\mu}{\mu_0}} = -\frac{g_i \mu_0 \eta_i}{2\pi^2} \int_{m_i}^{\infty} dE E \sqrt{E^2 - m_i^2} f_i(E), \quad (\text{A1})$$

$$\xrightarrow{T \rightarrow 0} -\frac{g_i \mu_0 \eta_i}{2\pi^2} \int_{m_i}^{\mu \eta_i} dE E \sqrt{E^2 - m_i^2}, \quad (\text{A2})$$

$$= -\frac{g_i \mu_0 \eta_i}{2\pi^2} \frac{1}{3} ((\mu \eta_i)^2 - m_i^2)^{\frac{3}{2}}. \quad (\text{A3})$$

Notice that at finite temperatures the quantity η_i is given by (cf. Eq. (2.17) and Sec. II C)

$$\eta_i = \begin{cases} 1 - (x_0 - \Delta x) & \text{if } i = u, c, \\ 1 & \text{if } i = d, s, \\ x_0 + \Delta x & \text{if } i = e^-, \mu^-. \end{cases} \quad (\text{A4})$$

All those quantities not defined here are explained in Sec. II. From Eq. (A3) one gets, using Eq. (2.18),

$$\left. \frac{\partial p_i}{\partial \frac{\Delta\mu}{\mu_0}} \right|_{\mu_0, x_0, T=0} = -\frac{g_i}{6\pi^2} \mu_0^4 n_i^4 (1 - z_i^2)^{\frac{3}{2}}. \quad (\text{A5})$$

The second coefficient reads

$$\frac{\partial p_i}{\partial \Delta x} = \frac{g_i c_i \mu}{2\pi^2} \int_{m_i}^{\infty} dE E \sqrt{E^2 - m_i^2} f_i(E) \quad (\text{A6})$$

$$\xrightarrow{T \rightarrow 0} \frac{g_i c_i \mu_0}{2\pi^2} \int_{m_i}^{\mu_0 \eta_i} dE E \sqrt{E^2 - m_i^2}, \quad (\text{A7})$$

and thus

$$\left. \frac{\partial p_i}{\partial \Delta x} \right|_{\mu_0, x_0, T=0} = \frac{g_i c_i}{6\pi^2} \mu_0^4 \eta_0^3 (1 - z_i^2)^{\frac{3}{2}}. \quad (\text{A8})$$

The third coefficient is obtained from

$$\frac{\partial p_i}{\partial \frac{T^2}{\mu_0^2}} = \frac{\mu_0^2 g_i}{12\pi^2} \left\{ \int_{-\infty}^{\infty} d\xi \xi (\xi T + \mu\eta_i)^3 \frac{e^\xi}{(1+e^\xi)^2 T} - \frac{3}{2} m_i^2 \int_{-\infty}^{\infty} d\xi \xi (\xi T + \mu\eta_i) \frac{e^\xi}{(1+e^\xi)^2 T} \right\}, \quad (\text{A9})$$

where the transformation $\xi \equiv (E - \mu\eta_i)/T$ has been introduced. For the zero-temperature coefficient one gets

$$\left. \frac{\partial p_i}{\partial \frac{T^2}{\mu_0^2}} \right|_{\mu_0, x_0, T=0} = \frac{\mu_0^2 g_i}{12\pi^2} \left\{ 3(\mu_0\eta_i)^2 \frac{\pi^2}{3} - \frac{3}{2} m_i^2 \frac{\pi^2}{3} \right\} \quad (\text{A10})$$

$$= \frac{g_i}{12} \mu_0^4 \eta_i^2 \left(1 - \frac{1}{2} z_i^2 \right). \quad (\text{A11})$$

The coefficients occurring in the expansion of particle density are obtained from Eq. (2.6), and are given by

$$\frac{\partial n_i}{\partial \frac{\Delta\mu}{\mu_0}} = -\frac{g_i \mu_0 \eta_i}{2\pi^2} \int_{\frac{m_i - \mu\eta_i}{T}}^{\infty} d\xi (\xi T + \mu\eta_i) \sqrt{(\xi T + \mu\eta_i)^2 - m_i^2} \frac{e^\xi}{(1+e^\xi)^2}, \quad (\text{A12})$$

$$\left. \frac{\partial n_i}{\partial \frac{\Delta\mu}{\mu_0}} \right|_{\mu_0, x_0, T=0} = -\frac{g_i \mu_0 \eta_i}{2\pi^2} \mu_0 \eta_i \sqrt{(\mu\eta_i)^2 - m_i^2} \int_{-\infty}^{\infty} d\xi \frac{e^\xi}{(1+e^\xi)^2}, \quad (\text{A13})$$

$$= -\frac{g_i}{2\pi^2} \mu_0^3 \eta_i^3 \sqrt{1 - z_i^2}, \quad (\text{A14})$$

and

$$\frac{\partial n_i}{\partial \Delta x} = \frac{g_i \mu c_i}{2\pi^2} \int_{\frac{m_i - \mu\eta_i}{T}}^{\infty} d\xi (\xi T + \mu\eta_i) \sqrt{(\xi T + \mu\eta_i)^2 - m_i^2} \frac{e^\xi}{(1+e^\xi)^2}, \quad (\text{A15})$$

which has the same mathematical structure as Eq. (A12). At zero temperature it reduces to

$$\left. \frac{\partial n_i}{\partial \Delta x} \right|_{\mu_0, x_0, T=0} = \frac{g_i c_i}{2\pi^2} \mu_0^3 \eta_i^2 \sqrt{1 - z_i^2}. \quad (\text{A16})$$

Finally, from

$$\frac{\partial n_i}{\partial \frac{T^2}{\mu_0^2}} = \frac{g_i \mu_0^2}{4\pi^2} \int_{\frac{m_i - \mu\eta_i}{T}}^{\infty} d\xi \frac{\xi}{T} (\xi T + \mu\eta_i) \sqrt{(\xi T + \mu\eta_i)^2 - m_i^2} \frac{e^\xi}{(1+e^\xi)^2}, \quad (\text{A17})$$

$$= \frac{g_i \mu_0^2}{4\pi^2} \left(\int_{-\infty}^{+\infty} d\xi \frac{\xi}{T} (\xi T + \mu\eta_i)^2 \frac{e^\xi}{(1+e^\xi)^2} - \frac{1}{2} \int_{-\infty}^{+\infty} d\xi \frac{\xi}{T} m_i^2 \frac{e^\xi}{(1+e^\xi)^2} \right), \quad (\text{A18})$$

one gets

$$\left. \frac{\partial n_i}{\partial \frac{T^2}{\mu_0^2}} \right|_{\mu_0, x_0, T=0} = \frac{g_i \mu_0^2}{2\pi^2} \mu_0 \eta_i \frac{\pi^2}{3} = \frac{g_i}{6} \mu_0^3 \eta_i. \quad (\text{A19})$$

The expansion coefficients of particle density enter in the condition of electric charge neutrality, Eq. (2.3), written at finite temperature:

$$0 = \sum_i q_i \left\{ n_{i,0} + \left. \frac{\partial n_i}{\partial \frac{\Delta\mu}{\mu_0}} \right|_{\mu_0, x_0, T_0} \frac{\Delta\mu}{\mu_0} + \left. \frac{\partial n_i}{\partial \Delta x} \right|_{\mu_0, x_0, T_0} \Delta x + \left. \frac{\partial n_i}{\partial \frac{T^2}{\mu_0^2}} \right|_{\mu_0, x_0, T_0} \frac{T^2}{\mu_0^2} \right\}. \quad (\text{A20})$$

Now, Eq. (A20) holds at all temperatures $T \geq 0$. In the special case of $T = 0$ one has $\Delta\mu = \Delta x = 0$, and thus it follows that $\sum_i q_i n_{i,0} = 0$, in agreement with Eq. (2.3). Since the sum of the remaining three terms on the right-hand side of Eq. (A20) must be equal to zero at any temperature different from zero, all three must possess

the same functional temperature dependence. We thus make the ansatz

$$\frac{\Delta\mu}{\mu_0} = a\pi^2 \left(\frac{T}{\mu_0} \right)^2 \quad \text{and} \quad \Delta x = b\pi^2 \left(\frac{T}{\mu_0} \right)^2. \quad (\text{A21})$$

Inserting Eq. (A21) in Eq. (A20) leads to an equation of the form

$$0 = \tilde{A} a + \tilde{B} b - \tilde{Q} , \quad (\text{A22})$$

where

$$\begin{aligned} \tilde{A} &\equiv \pi^2 \sum_i q_i \left. \frac{\partial n_i}{\partial \frac{\Delta \mu}{\mu_0}} \right|_{\mu_0, x_0, T=0} \\ &= 1 - \sqrt{1 - z_s^2} - 3x_0(x_0^2 - 2x_0 + 2) \\ &\quad + 2(1 - x_0)^3 \sqrt{1 - z_c^2} - x_0^3 \sqrt{1 - z_\mu^2} , \end{aligned} \quad (\text{A23})$$

$$\begin{aligned} \tilde{B} &\equiv \pi^2 \sum_i q_i \left. \frac{\partial n_i}{\partial \Delta x} \right|_{\mu_0, x_0, T=0} \\ &= 2 - x_0(4 - 3x_0) + 2(1 - x_0)^2 \sqrt{1 - z_c^2} \\ &\quad + x_0^2 \sqrt{1 - z_\mu^2} , \end{aligned} \quad (\text{A24})$$

$$\begin{aligned} \tilde{Q} &\equiv - \sum_i q_i \left. \frac{\partial n_i}{\partial \frac{T^2}{\mu_0^2}} \right|_{\mu_0, x_0, T=0} \\ &= \frac{1}{3} (1 - 5x_0) . \end{aligned} \quad (\text{A25})$$

To derive the pressure-energy density relation at finite temperature, we start from Eq. (2.1), which reads now (p denotes an external pressure acting on the quark bag)

$$p + B = \sum_i \left[p_{i,0} + \left\{ \left. \frac{\partial p_i}{\partial \frac{\Delta \mu}{\mu_0}} \right|_{\mu_0, x_0, T_0} \frac{\Delta \mu}{\mu_0} + \left. \frac{\partial p_i}{\partial \Delta x} \right|_{\mu_0, x_0, T_0} \Delta x + \left. \frac{\partial p_i}{\partial \frac{T^2}{\mu_0^2}} \right|_{\mu_0, x_0, T_0} \frac{T^2}{\mu_0^2} \right\} \right] . \quad (\text{A26})$$

Since at zero temperature $p + B = \sum_i p_{i,0}$, it follows that the expansion in curly brackets must vanish identically. By means of Eq. (A21) one obtains, in analogy with Eq. (A22),

$$0 = \tilde{C} a + \tilde{D} b - \tilde{P} , \quad (\text{A27})$$

where

$$\begin{aligned} \tilde{C} &\equiv \pi^2 \sum_i \left. \frac{\partial p_i}{\partial \frac{\Delta \mu}{\mu_0}} \right|_{\mu_0, x_0, T=0} \\ &= (1 - x_0)^4 + \frac{1}{3} x_0^4 + 1 + (1 - z_s^2)^{\frac{3}{2}} + (1 - x_0)^4 (1 - z_c^2)^{\frac{3}{2}} + \frac{1}{3} x_0^4 (1 - z_\mu^2)^{\frac{3}{2}} , \end{aligned} \quad (\text{A28})$$

$$\begin{aligned} \tilde{D} &\equiv \pi^2 \sum_i \left. \frac{\partial p_i}{\partial \Delta x} \right|_{\mu_0, x_0, T=0} \\ &= (1 - x_0)^3 - \frac{1}{3} x_0^3 + (1 - x_0)^3 (1 - z_c^2)^{\frac{3}{2}} - \frac{1}{3} x_0^3 (1 - z_\mu^2)^{\frac{3}{2}} , \end{aligned} \quad (\text{A29})$$

$$\begin{aligned} \tilde{P} &\equiv - \sum_i \left. \frac{\partial p_i}{\partial \frac{T^2}{\mu_0^2}} \right|_{\mu_0, x_0, T=0} \\ &= \frac{1}{2} \left[(1 - x_0)^2 + 1 + (1 - \frac{1}{2} z_s^2) + \frac{1}{3} x_0^2 + (1 - x_0)^2 (1 - \frac{1}{2} z_c^2) + \frac{1}{3} x_0^2 (1 - \frac{1}{2} z_\mu^2) \right] . \end{aligned} \quad (\text{A30})$$

Muons and c quarks occur in the system only at densities larger than $3.8 \times 10^{17} \text{ g/cm}^3$ and $1.1 \times 10^{17} \text{ g/cm}^3$, respectively. Quark matter at lower densities consists of only u, d, s , quarks and electrons. For such matter the above coefficients, \tilde{A} through \tilde{P} , are given by the simpler relations

$$\tilde{A} = 1 - \sqrt{1 - z_s^2} - 3x_0(x_0^2 - 2x_0 + 2) , \quad (\text{A31})$$

$$\tilde{B} = 2 - x_0(4 - 3x_0) , \quad (\text{A32})$$

$$\tilde{Q} = -x_0 , \quad (\text{A33})$$

$$\tilde{C} = (1 - x_0)^4 + \frac{1}{3} x_0^4 + 1 + (1 - z_s^2)^{\frac{3}{2}} , \quad (\text{A34})$$

$$\tilde{D} = (1 - x_0)^3 - \frac{1}{3} x_0^3 , \quad (\text{A35})$$

$$\tilde{P} = \frac{1}{2} \left[(1 - x_0)^2 + 1 + (1 - \frac{1}{2} z_s^2) + \frac{1}{3} x_0^2 \right] . \quad (\text{A36})$$

Equations (A22) and (A27) constitute two relations for the two unknowns a and b . Solving for them and inserting the results into Eqs. (2.33) and (A21) leads to the expressions for p_i and n_i given by Eqs. (2.34) and (2.35), respectively. Finally, the expression for the energy density is obtained from Eqs. (2.1) and (2.2) which, for this purpose, are combined to

$$\epsilon = 3p + 4B + \sum_{i=c,s,\mu^-} (\epsilon_i - 3p_i) . \quad (\text{A37})$$

- [1] A. R. Bodmer, *Phys. Rev. D* **4**, 1601 (1971).
- [2] E. Witten, *Phys. Rev. D* **30**, 272 (1984).
- [3] E. Farhi and R. L. Jaffe, *Phys. Rev. D* **30**, 2379 (1984).
- [4] N. K. Glendenning, *Mod. Phys. Lett. A* **5**, 2197 (1990).
- [5] G. Baym, E. W. Kolb, L. McLerran, T. P. Walker, and R. L. Jaffe, *Phys. Lett.* **160B**, 181 (1985).
- [6] C. Alcock, E. Farhi, and A. Olinto, *Phys. Rev. Lett.* **16**, 2088 (1986).
- [7] A. V. Olinto, *Phys. Lett. B* **192**, 71 (1987).
- [8] C. Alcock and A. V. Olinto, *Annu. Rev. Nucl. Part. Sci.* **38**, 161 (1988).
- [9] N. K. Glendenning, *Strange-Quark-Matter Stars*, in Proceedings of the International Workshop on Relativistic Aspects of Nuclear Physics, Rio de Janeiro, Brazil, 1989, edited by T. Kodama, K. C. Chung, S. J. B. Duarte, and M. C. Nemes (World Scientific, Singapore, 1990).
- [10] P. Haensel, B. Paczynski, and P. Amsterdamski, *Astrophys. J.* **375**, 209 (1991).
- [11] J. Madsen, *Physics and Astrophysics of Strange Quark Matter*, in Proceedings of the 2nd International Conference on Physics and Astrophysics of Quark-Gluon Plasma, Calcutta, India, 1993, edited by B. Sinha, Y. P. Viyogi, and S. Raha (World Scientific, Singapore, 1994).
- [12] J. E. Horvath, H. Vucetich, and O. G. Benvenuto, *Mon. Not. R. Astron. Soc.* **262**, 506 (1993).
- [13] *Strange Quark Matter in Physics and Astrophysics*, Proceedings of the International Workshop, Aarhus, Denmark, 1991, edited by J. Madsen and P. Haensel [*Nucl. Phys. B (Proc. Suppl.)* **24B** (1991)].
- [14] C. Alcock, E. Farhi, and A. V. Olinto, *Astrophys. J.* **310**, 261 (1986).
- [15] P. Haensel, J. L. Zdunik, and R. Schaeffer, *Astron. Astrophys.* **160**, 121 (1986).
- [16] P. Haensel and J. L. Zdunik, in *Strange Quark Matter in Physics and Astrophysics* [13], p. 139.
- [17] N. K. Glendenning and F. Weber, *Astrophys. J.* **400**, 647 (1992).
- [18] N. K. Glendenning, *Supernovae, Compact Stars, and Nuclear Physics*, invited paper in Proceedings of the 1989 International Nuclear Physics Conference, São Paulo, Brazil, Vol. 2, edited by M. S. Hussein *et al.* (World Scientific, Singapore, 1990).
- [19] F. Weber and N. K. Glendenning, *Astrophys. J.* **390**, 541 (1992).
- [20] F. Weber and N. K. Glendenning, *Impact of the Nuclear Equation of State on Models of Rotating Neutron Stars*, in Proceedings of the International Workshop on Unstable Nuclei in Astrophysics, Tokyo, Japan, 1991, edited by S. Kubono and T. Kajino (World Scientific, Singapore, 1992).
- [21] F. Weber and N. K. Glendenning, *Hadronic Matter and Rotating Relativistic Neutron Stars*, in Proceedings of the Nankai Summer School, "Astrophysics and Neutrino Physics," Tianjin, China, 1991, edited by D. H. Feng, G. Z. He, and X. Q. Li (World Scientific, Singapore, 1993), pp. 64–183.
- [22] F. Weber and N. K. Glendenning, *Neutron Stars, Strange Stars, and the Nuclear Equation of State*, in Proceedings of the First Symposium on Nuclear Physics in the Universe, edited by M. W. Guidry and M. R. Strayer (IOP, Bristol, 1993), p. 127.
- [23] N. K. Glendenning, *Nuclear and Particle Astrophysics*, in Proceedings of the International Summer School on the Structure of Hadrons and Hadronic Matter, Dronthon, Netherlands, 1990, edited by O. Scholten and J. H. Koch (World Scientific, Singapore, 1991), p. 275.
- [24] A. Chodos, R. L. Jaffe, K. Johnson, C. B. Thorne, and V. F. Weisskopf, *Phys. Rev. D* **9**, 3471 (1974).
- [25] T. Chmaj and W. Słominski, *Phys. Rev. D* **40**, 165 (1988).
- [26] B. A. Freedman and L. D. McLerran, *Phys. Rev. D* **16**, 1130 (1977); **16**, 1147 (1977); **16**, 1169 (1977).
- [27] B. A. Freedman and L. D. McLerran, *Phys. Rev. D* **17**, 1109 (1978).
- [28] A. Burrows, *Astrophys. J.* **335**, 891 (1988).
- [29] E. Müller, *J. Phys. G* **16**, 1571 (1990).
- [30] J. Cooperstein and E. Baron, in *Supernovae*, edited by A. Petschek (Springer-Verlag, Berlin, 1990).
- [31] Ch. Kettner, "Struktur und Stabilität von Quark-Sternen," diploma thesis, University of Munich, F.R.G., 1994.
- [32] B. K. Harrison and J. A. Wheeler, cited in *Gravitation Theory and Gravitational Collapse*, edited by B. K. Harrison, K. S. Thorne, M. Wakano, and J. A. Wheeler (University of Chicago Press, Chicago, 1965).
- [33] C. W. Misner and H. S. Zepolsky, *Phys. Rev. Lett.* **12**, 635 (1964).
- [34] G. Baym, C. Pethick, and P. Sutherland, *Astrophys. J.* **170**, 299 (1971).
- [35] J. Madsen, *Phys. Rev. D* **46**, 3290 (1992).
- [36] J. R. Oppenheimer and G. M. Volkoff, *Phys. Rev.* **55**, 374 (1939).
- [37] N. K. Glendenning, Ch. Kettner, and F. Weber, "From Strange Stars to Strange Dwarfs," Report No. LBL-34869, 1993 (unpublished).
- [38] J. M. Bardeen, K. S. Thorne, and D. W. Meltzer, *Astrophys. J.* **145**, 505 (1966).
- [39] S. L. Shapiro and S. A. Teukolsky, *Black Holes, White Dwarfs, and Neutron Stars* (Wiley, New York, 1983).
- [40] B. Datta, P. K. Sahu, J. D. Anand, and A. Goyal, *Phys. Lett. B* **283**, 313 (1992).
- [41] H. M. Vät and G. Chanmugam, *Astron. Astrophys.* **260**, 250 (1992).